Published in final edited form as:
Nanomedicine (Lond). 2011 June ; 6(4): 605–615. doi:10.2217/nnm.11.21.

A fibrin-specific thrombolytic nanomedicine approach to acute ischemic stroke

Jon N Marsh[1], **Grace Hu**[1], **Michael J Scott**[1], **Huiying Zhang**[1], **Matthew J Goette**[2], **Patrick J Gaffney**[3], **Shelton D Caruthers**[1], **Samuel A Wickline**[1,2], **Dana Abendschein**[1], and **Gregory M Lanza**[1,2,†]

[1]Washington University School of Medicine, St Louis, MO, USA

[2]Department of Biomedical Engineering, Washington University, St Louis, MO, USA

[3]Academic Department of Surgery, Guy's St Thomas' NHS Foundation Trust, London, UK

Abstract

Aim—To develop a fibrin-specific urokinase nanomedicine thrombolytic agent.

Materials & Methods—*In vitro* fibrin-clot dissolution studies were utilized to develop and characterize simultaneous coupling and loading of anti-fibrin monoclonal antibody and urokinase onto perfluorocarbon nanoparticle (NP) surface. *In vivo* pharmacokinetics and fibrin-specific targeting of the nanolytic agent was studied in dogs.

Results—Simultaneous coupling of up to 40 anti-fibrin antibodies and 400 urokinase enzymes per perfluorocarbon NP produced an effective targeted nanolytic agent with no significant surface protein–protein interference. Fibrin clot dissolution was not improved by increasing homing capacity from 10 to 40 antibodies/NP, but increasing enzymatic payload from 100 to 400/NP resulted in maximized lytic effect. Fluorescent microscopy showed that rhodamine-labeled urokinase nanoparticles densely decorated the intraluminal thrombus in canine clots *in vivo* analogous to the fibrin pattern, while an irrelevant-targeted agent had negligible binding.

Conclusion—This agent offers a vascularly constrained, simple to administer, low-dose nanomedicine approach that may present an attractive alternative for treating acute stroke victims.

Keywords

emergency treatment of stroke; nanoparticle; perfluorocarbon; targeted thrombolysis; urokinase

Stroke is the third leading cause of death and most common etiology for long-term adult disability. Of the approximate 700,000 individuals suffering from new or recurrent stroke

†Author for correspondence: Tel.: +1 314 454 8635, Fax: +1 314 454 5265, greg@cvu.wustl.edu.

Ethical conduct of research

The authors state that they have obtained appropriate institutional review board approval or have followed the principles outlined in the Declaration of Helsinki for all human or animal experimental investigations. In addition, for investigations involving human subjects, informed consent has been obtained from the participants involved.

Financial & competing interests disclosure

The article was supported by NINDS (R01NS059302) and NHLBI (R01HL094470). Equipment was provided by Philips Healthcare. Technology described in this manuscript is owned by Washington University (WA, USA) and is licensed to Kereos, Inc. However, this concept is not currently under commercial development for translation to the clinic. SAW and GML are scientific cofounders of Kereos, Inc. The authors have no other relevant affiliations or financial involvement with any organization or entity with a financial interest in or financial conflict with the subject matter or materials discussed in the manuscript apart from those disclosed.
No writing assistance was utilized in the production of this manuscript.

annually, less than 5% of these individuals receive thrombolytic therapy [1–3]. The evidence from PET studies has revealed that early reperfusion, either spontaneous or chemically initiated, primarily determines the final size of brain infarction; these hypoperfused regions account for the majority of the final infarct volume [4].

Systemic therapy with intravenous tissue plasminogen activator (tPA) was approved in the USA after the pivotal trial demonstrated a 6.4% symptomatic hemorrhage rate [5]. Subsequent trials in Europe showed even lower rates of clinically relevant brain hemorrhagic complications and provided evidence for extension of the time window up to 4.5 h from symptom onset [6,7]. We anticipate that a nanomedicine approach could further reduce associated complication rates by focusing enzymatic treatment and lowering the overall systemic dose of thrombolytic agents.

Perfluorocarbon (PFC) nanoparticles, previously considered as artificial blood substitutes [8,9], have been developed into a platform technology for molecular imaging and targeted drug delivery. These lipid-encapsulated particles, nominally 250 nm in diameter, are administered intravenously and constrained by size within blood vessels, including the ‘leaky’ neovasculatures associated with cancer, atherosclerotic disease and inflammatory arthritis [10–13]. We hypothesize that fibrin-targeted PFC nanoparticles, each presenting hundreds of fibrinolytic enzyme molecules on the surface, could be easily administered as an intravenous rider, allowing the particles to circulate to the intra-arterial thrombus and to begin recanalizing the obstruction with the generation of plasmin intimately approximated to the fibrin fibrils. Constraint of the particle-bound fibrinolytic activity to the circulatory system and reticuloendothelial clearance of the unbound thrombolytic nano-particles is expected to minimize hemorrhagic complications from extravascular or untargeted enzyme activity, providing a more sophisticated and effective intervention [14].

We have reported that streptokinase can be covalently bonded to the surface of a PFC nanoparticle, which can be targeted to clots and effect their rapid dissolution *in vitro* [15]. The objective of the present study was to extend this research by: assessing the effectiveness of covalently modified human urokinase as a substitute for streptokinase coupled to the nanoparticle surface; and characterizing and demonstrating the simultaneous presentation of the enzymes and homing ligands on the nanoparticle surface for targeted thrombolytic activity.

Materials & methods

Preparation of fibrin-specific thrombolytic nanoparticles Synthesis of nanoparticles

Nanoparticles were comprised of 20% (v/v) perfluorooctylbromide (PFOB; Exfluor Research, TX, USA) and 2.0% (w/v) of a surfactant comixture, 1.7% (w/v) glycerin and water for the balance. The surfactant comixtures variably included approximately 68 mole% highly purified egg yolk lecithin (Avanti Polar Lipids, Inc, AL, USA), 1.0 mol% 1,2-dipalmitoylsn glycero-3-phosphoethanolamine-*N*-4-(p-maleimidophenyl) butyramide (MPB-PE; Avanti Polar Lipids) for coupling *N*-succinimidyl-*S*-acetylthioacetate (SATA)-derivatized proteins. For fluorescent microscopy, 0.3 mol% rhodamine-phosphatidylethanolamine was included in the surfactant comixture. The surfactant components were dissolved in chloroform/methanol, evaporated under reduced pressure, dried in a 50°C vacuum oven overnight and dispersed into water by sonication. The nominal sizes for the derivatized PFC nanoparticle formulations were determined with a Zeta Plus light-scattering particle analyzer (Brookhaven Instruments Corporation, NY, USA). Nanoparticle number was estimated from the nominal particle volume and the PFC volume concentration.

Modification & coupling of fibrinolytic enzymes & homing ligands

Fibrinolytic enzymes were derivatized for covalent coupling by combining with SATA in dimethylsulfoxide (DMSO) (Pierce, Inc., IL, USA). Specifically, 100 mg urokinase (Cell Sciences, Inc., MA, USA) or streptokinase (Sigma-Aldrich, MO, USA) in 7 ml buffer (0.5 M ammonium hydroxyl in 0.1 M phosphate-buffered saline [PBS] with 10 mM ethylenediaminetetraacetic acid; pH 7.0) was mixed with 100 μl 0.037 M SATA (2.2 mg SATA per 255 μl DMSO for 30–40 min). Following dialysis against PBS buffer (pH 7.0) to remove unreacted SATA, the modified enzyme was treated with 1.16 ml 0.5 M NH_2OH for 2 h at room temperature (RT).

Anti-fibrin monoclonal antibodies were produced and purified from hybridoma by conventional methods. The National Institute of Biological Standards and Controls, London (NIBSC) antibody (NIB 1H10) was thoroughly characterized and reported to have 10^{-10} M affinity for human, canine and porcine fibrin with no cross-reactivity to fibrinogen [16–18]. SATA was modification of 1H10 or irrelevant IgG_1 as follows: 16 mg of antibody in 2.76 ml PBS (pH 7.0) was reacted with 5.3 μl of 0.037 M SATA in DMSO (as above) for 30 min at RT. The SATA-modified antibody mixture dialyzed against PBS was reduced with 61.9 μl of 0.5 M NH_2OH at RT for 2 h.

N-succinimidyl-*S*-acet ylthioacetate-modified urokinase or streptokinase and or SATA-modified 1H10 were mixed with MPB-PEG-PE incorporated nanoparticles at RT for 2 h to produce the desired coupling to nanoparticle ratios. Enzyme or antibody mass per particle was estimated from the uncoupled concentrations in the excipient before dialysis determined by high-performance liquid chromatography subtracted from the total amount of compound applied, then normalized by the number density of particles. Free MPB remaining on the nanoparticle surface was reacted with cysteine and unconjugated protein was removed by dialysis. A high-performance liquid chromatograph (Waters Corporation, MA, USA) with UV detection was employed to assess the coupling of enzyme and ligand to the per-fluorocarbon nanoparticles. In these determinations, the emulsion was centrifuged and the supernatant was analyzed by high performance liquid chromatography using a linear gradient: the mobile phase was (A) 0.05 M triethylamine phosphoric in water, pH 2.6 and (B) 100% acetonitrile. The gradient was 0–1 min 0%B, 1–12 min 0– 50%B, 12–15 min 50%B, then re-equilibrated to 0%B for 15–30 min. A Waters Symmetry™ RP8 column, 4.6 × 150 mm 3.5-μm pH range 2–8 was used with 1 ml/min flow rate at 25°C column temperature and UV detection at 215 nm. Coupling efficiencies exceeded 90%. Final particle size after coupling antibody and enzymes (ZetaPlus, Brookhaven Instruments Corporation) was 354-nm nominal diameter (polydispersity 0.33).

In vitro clot sample preparation & measurements Fibrin clot formation

Acellular thrombi were produced from citrated human plasma combined with 500 mM and thrombin (3 U/μl). For acoustic $CaCl_2$ microscopy, each clot was formed by quickly dispensing 90 μl of this mixture onto a nitro-cellulose membrane substrate (1 × 2 cm) and allowing this mixture to coagulate for 2 min before immersion in PBS. For optical measurements, small cylindrical clots (~5 mm diameter, 10 mm long) were formed in tubular templates from approximately 200 μl of a similar clot mixture. After 2 min of coagulation, each clot was removed from the template and immersed in 5 ml PBS individually in a six-well cluster plate. All clots were maintained at 4°C overnight in PBS and rinsed with at least three changes of PBS to elute out intrinsic plasminogen before exposure to nanoparticles.

Acoustic microscopy for assessment of fibrin targeting & lysis

Acoustic microscopy was performed on clot samples using a custom apparatus [15] with a 25-MHz transducer affixed to a motorized gantry (Figure 1A). Backscatter data were acquired at every site, as the transducer was scanned over each sample in a rectangular grid with 250-μm resolution. Samples were sealed within a PBS-filled chamber having a cellophane acoustic window. The chamber was submerged in a 37°C waterbath and fixed in position for scanning. After a baseline scan, the chamber was emptied of PBS and refilled with 3 U/ml plasminogen solution (Calbiochem, CA, USA). Scans were then performed at 30-min intervals for up to 3 h, and spatial registration was maintained at all times. Prior to each scan, the sample chamber was removed from the waterbath and placed on a shaker table to gently agitate the specimens at 100 rpm for 1 min.

Radiofrequency data were analyzed to assess temporal changes in clot morphology and backscatter (Figure 1B & 1C). The difference between the echo arrival times from the clot surface and substrate determined the profile of the clot for computation of the sample volume.

Optical digital imaging & analysis for assessment of fibrin targeting & lysis

Cylindrical clots formed as described above were immersed in PBS solution in six-well plates and photographed with visible light against a dark background using a high-resolution digital imaging system (MultiDoc-It, Ultraviolet Products, CA, USA). A baseline image was acquired from the samples before treatment; images were then taken at 30-min intervals for up to 3 h subsequent to exposure to lytic agents. Example images of a clot targeted with urokinase-loaded nanoparticles at baseline and after 2 h exposure to plasminogen are shown in FIGURE 2. Clot volumes at each time point were estimated from photographic images using a custom Java routine to generate a best-fit rectangle to the clot boundary. Under the assumption that the clots maintained an approximately cylindrical shape (borne out by visual observation), clot volume was estimated from the dimensions of the rectangle.

In vitro experimentation to characterize & optimize fibrinolytic nanoagent Effect of SATA modification on urokinase activity

The dissolution of plasma clots following the SATA modification at nominally none, three and six sites was performed as described above. Thrombi in triplicate were exposed to the SATA-modified urokinase (0.1 mg enzyme per clot) in the presence of excess plasminogen at 37°C. Acoustic microscopy was used to assess the residual clot volumes over 3 h in 30-min intervals.

Impact of surface antibody number of nanoparticle binding in the presence of urokinase

Perfluorocarbon nanoparticles were cofunctionalized with anti-fibrin monoclonal antibodies to achieve nominal levels of zero, ten, 20 and 40 ligands simultaneously with the incorporation of nominally 100 urokinase enzymes (3:1 SATA-modified sites:enzyme) per nano-particle. Thrombi in triplicate were exposed to the PFC nanoparticles for 1 h at 37°C. After incubation, unbound particles were washed away with PBS and plasminogen (3 U/ml) was introduced. Acoustic microscopy was used to assess the residual clot volumes over 2 h in 30-min intervals.

Impact of increasing fibrinolytic enzyme density per fibrin-targeted PFC particle on clot dissolution

Using 20 antibodies/particle based on experiment two, the number of fibrinolytic enzymes (3:1 SATA-modified urokinase and streptokinase) was varied at levels of 100, 200 and 400 per particle. As above, thrombi, studied in triplicate, were exposed to the PFC nanoparticles

presenting urokinase or streptokinase at 37°C, and optical digital analysis was used to assess the fractional clot remaining over 120 min.

Comparison of the rate of fibrin-targeted fibrinolytic PFC nanoparticle dissolution & equivalent SATA-modified free enzyme dissolution rate

Rate of clot digestion (%/min) was compared between fibrinolytic enzyme functionalized fibrin-targeted PFC nanoparticles (400:20 urokinase: or streptokinase:antibody) and the respective 3:1 SATA-modified fibrinolytic enzymes. The volume of free enzyme solution or fibrin-targeted lytic nanoparticle emulsion added to each clot well was adjusted to ensure the same total amount of enzyme (0.1 mg enzyme/clot) was applied for all samples. Clots exposed to targeted nanoparticles were washed of unbound agent after 1 h incubation; however, free enzyme was allowed to remain with the clot for the entire experiment. Optical digital analysis was used to assess the fractional clot volume remaining after 120 min, from which continuous digestion rates were estimated by interpolation between time points. Fractional clot remaining was modeled over time using these rates.

In vivo clot generation & fibrin-targeted urokinase nanoparticles in dogs

Animals were studied under a protocol approved by the Washington University Animal Studies Committee. Beagles (9–10 kg; n = 6) were pre-medicated before sedation with Telazol® cocktail (1 ml/23 kg intramuscularly) followed by intubation and 1–2% isoflurane anesthesia in oxygen. Animals were hydrated with a solution of 1% tranexamic acid in normal saline to inhibit enzymatic fibrinolysis (endogenous or exogenous). Vascular injury was induced by a transmural electrode inserted into and secured to the femoral artery. Blood flow distal to the injury was monitored continuously using an ultrasonic flow probe (TS420, Transonic Systems, NY, USA). Clot induction was continued in flowing blood until flow was reduced to 0 ml/s. Fibrin-targeted or irrelevant IgG targeted urokinase nanoparticles (200:20 urokinase:antibody ratio) were injected via catheter intravenously through the contralateral femoral vein (2 ml/kg). Femoral artery segments were excised 2 h post-nanoparticle injection and quick frozen for subsequent histological evaluation of particle-fibrin binding.

Statistical analysis

Changes in clot volume (transformed to log domain) were assessed within each sampling time and over time using two-way and repeated measures general linear models in SAS (SAS Institute, NC, USA). The main effects with significant ($p < 0.05$) F-tests (Type III SS) were compared using least square means to account for occasional unequal subclass numbers. Data are presented as the arithmetic mean ± standard error of the mean.

Results

The sensitivity of urokinase to SATA modification is shown in Figure 3. The sulfhydryl functionalization of urokinase with SATA significantly decreased the overall enzymatic activity of free urokinase, which was reflected as a slightly slower initial clot dissolution rate in the presence of excess human plasminogen. However, the overall bioactivity was not reduced markedly.

The effect of steric inhibition on urokinase bioactivity due to antibody presentation density was evaluated by titrating the nominal number of antibodies at zero, ten, 20 and 40 simultaneously coupled with 100 urokinase molecules presenting 0:10, 100:10, 100:20 or 100:40 urokinase:antibody per particle. The overall dissolution of plasma clots with the urokinase-functionalized particles was significantly greater than the control group, regardless of the number of antibodies coupled to the surface as expected (Figure 4),

indicating that urokinase activity was uncompromised and equally effective with ten to 40 antibodies per particle.

However, the overall fibrinolytic activation activity achieved was lower than desired with 100 urokinase molecules per particle. Selecting the midpoint 20-antibody density, anticipating more stringent conditions ultimately *in vivo* than *in vitro*, the number of fibrinolytic enzymes per particle was titrated upward to 400 per particle. Moreover, the differential effectiveness of urokinase and previously reported streptokinase was assessed. As shown in Figure 5, urokinase and strep-tokinase nanoparticles targeted to the plasma clots induced fibrinolysis. Analyzed over all enzyme densities, urokinase nanoparticles attained significantly more effective clot dissolution than the streptokinase counterparts. Higher presentation numbers of enzymes per particle monotonically produced increased levels of lysis. For streptokinase particles, the increase in enzyme density significantly improved clot dissolution measured at 120 min at each level of titration ($p < 0.05$). Among the urokinase nanoparticle formulations, presentation of 200 and 400 enzymes per particle similarly increased ($p < 0.05$) clot dissolution relative to the 100-urokinase nanoparticles, but there was no lytic difference observed between the two higher enzyme densities.

Comparison of the rates of clot dissolution for fibrin-targeted streptokinase and urokinase functionalized nanoparticles (400:20) with the equivalent concentration of free 3:1 SATA-functionalized enzymes is shown in Figure 6A. Average rates of lysis for the urokinase nano-particles and the free enzyme were similar ($p > 0.05$) over 150 min. In contradistinction, ANOVA revealed a significant ($p < 0.05$) interaction between the nanoparticle-based and free enzyme lysis rates for streptokinase. Fibrin-targeted streptokinase nanoparticles had significantly higher early dissolution rate (30 min) than the free enzyme, but beyond 60 min, the overall effectiveness of the targeted streptokinase nanoparticles was lower ($p < 0.05$) than the free enzyme rate of clot lysis. The free SATA-modified streptokinase clot dissolution rate did not differ ($p > 0.05$) from the urokinase-based groups.

Although the total amount of enzyme initially added to the clot wells prior to plasminogen exposure was equivalent for both free fibrinolytic enzymes and fibrin-specific nanoparticle–enzyme conjugates, the unbound nanoparticles were washed from the wells, greatly lowering the total enzyme exposure, while the free enzyme remained unchanged. Thus, the net amount of lytic enzyme concentrated by the targeted particles was substantially less than the free enzyme level in the well. Nevertheless, the digestion rate upon introduction of plasminogen was approximately equivalent to samples exposed to free enzyme, confirming the high retention of enzymatic activity on the nanoparticles and illustrating the large potential benefit afforded by targeting fibrin specifically. Modeling the rate data (Figure 6B) illustrates that after 30 min, both urokinase groups and the fibrin-targeted strep-tokinase nanoparticles diminished clot volume by 40%, which could be an adequately rapid result to ameliorate acute cerebral ischemia.

Having demonstrated and characterized the fibrinolytic activation activity of the urokinase nanoparticles *in vitro*, characterization of the nanoagent's *in vivo* binding to thrombus was needed to adequately demonstrate the concept. Fibrin-targeted urokinase nanoparticle or non-specifically targeted urokinase nanoparticles (200:20) were injected into the contralateral femoral vein of dogs and allowed to circulate for 2 h. Microscopic examination of the resected thrombus, presented in Figure 7, demonstrated effective targeting of fibrin by the 1H10-guided particles and no binding to clot by the irrelevantly homed agent. Hematoxylin and eosin (H&E)-stained femoral artery segments in Figure 7A & 7B, for the irrelevant-targeted and fibrin-targeted particles, respectively, show anodal injury induced thrombus attached to the femoral wall. During the formation of both thrombi, the ultrasonic

flow probe distal to the injury site measured no blood flow, but microscopic examination revealed only partial occlusion, indicating that some thrombus was lost in the resection, washing and processing of tissue for microscopy. Figure 7B was fortuitously obtained near the needle injury site and revealed disruption of the intima and internal elastic lamina (highlighted with arrows in Figure 7D & 7F). Carstair's staining of fibrin, Figure 7C & 7D, revealed an abundance of the target protein in both thrombi. Fluorescent microscopic examinations of the thrombi that show the fibrin-targeted urokinase nanoparticles labeled with rhodamine (Figure 7F) were bound along the serpentine surface of thrombus in a pattern consistent with the fibrin deposits revealed by the Carstair's stain in Figure 7D. In contradistinction, only negligible binding of the irrelevant-targeted urokinase particles labeled with rhodamine was observed (Figure 7E), despite a prominent accumulation of the target protein shown in Figure 7C. These data demonstrate that the fibrin (1H10)-targeted urokinase nanoparticles retain specific, high binding affinity when administered intravenously in a large animal model. Of further interest was the intense rhodamine signal obtained from the minute fibrin deposits, con-firmed by Carstair's stain, associated with the ruptured intima. This observation suggests that the homing of the fibrinolytic nanoparticles was not limited to targeting large intraluminal thrombus, but was very effective for targeting small mural microthrombus, similar to those anticipated with acutely ruptured plaque.

Discussion

Reperfusion of the ischemic brain is the most effective therapy for acute stroke, restoring nutrition and oxygen-rich blood flow to threatened tissues. The recommended treatment of stroke with recombinant tPA (r-tPA), is currently the best approach to treatment of patients presenting with acute ischemic stroke, but the use of this lytic agent can also worsen the disease through symptomatic and fatal hemorrhage complications. In one key report, r-tPA was associated with a 6.4% rate of symptomatic intracerebral hemorrhage versus 0.6% incidence in the placebo control group. From this group, approximately 50% died before discharge and of the surviving patients, approximately 50% had residual neurological deficit [5]. Although a more recent study confirmed that intravenous alteplase was safe and effective in routine clinical use when used within 3 h of stroke onset, even by centers with little previous experience of thrombolytic treatment for acute stroke [19], late arrival of patients to the emergency room and physician misconceptions toward stroke treatment has diminished the general clinical use of r-tPA to less than 5% of acute ischemic stroke patients [1,20]. A clear unmet need exists for an improved thrombolytic approach with less intracerebral hemorrhage risk in order to encourage greater treatment rates among acute stroke victims.

From a small molecule approach, a variety of novel fibrinolytic agents have been developed with greater fibrin specificity, longer half-life, and increased resistance to PAI-1 inactivation than r-tPA. These include tenecteplase [21], des-metoplase [22,23], reteplase [24], plasmin [25] and microplasmin [26]. Unfortunately, none clearly provides a substantial improvement over tPA with regard to safety or efficacy. Plasmin and microplasmin, a truncated form of the bioactive β-chain of plasmin, act directly on fibrin but they can be rapidly inactivated by circulating antiplasmin and should be delivered locally through an interventional radiology procedure.

Sonothrombolysis, an experimental technique where ultrasound is applied to enhance enzymatic thrombolysis alone or in the presence of microbubbles [27–31], is associated with higher rates of recanalization. In the Combined Lysis of Thrombus in Brain ischemia with Transcranial Ultrasound and Systemic TPA (CLOTBUST), Phase II multicenter randomized trial, ultrasound in combination with tPA did induce recanalization or dramatic clinical improvement in 49% of treated patients versus 29% of control patients. In a Phase II trial of

Transcranial Ultrasound in Clinical Sonolysis (TUCSON), stroke patients given r-tPA along with perflutren microspheres showed a trend toward higher early recanalization rates, but at higher microbubble doses the study was stopped due to safety concerns related to incidence of symptomatic intracerebral hemorrhage [31]. Very early *in vitro* results from a related r-tPA microbubble approach using an Arg–Gly–ASP–Ser (RGDS) ligand to target activated platelets in thrombus has been reported, which may ultimately offer improved homing specificity with lower microbubble and fibrinolytic dosages [32]. A similar ultrasound disruption approach using echogenic liposomes incorporating r-tPA has been reported *in vitro* and may offer clinical benefit, since these low gas-content particles may be less prone to illicit cavitation-induced side effects [33–35]. In contradistinction to the use of a directed ultrasound beam to provide external targeting of fibrinolytic payload release, two recent reports have used magnetic field guidance of urokinase-coupled to dextran-coated iron oxide particles or r-tPA coupled to polyacrylic acid-coated particles to enhance thrombotic delivery of lytic activity *in vitro* and in rat models of thrombosis [36,37].

In 2007, we hypothesized that fibrin-targeted thrombolytic PFC nanoparticles have the potential to deliver fibrinolytic therapy and dissolve cerebrovascular occlusions at lower doses of drug and with less hemorrhagic risk than free thrombolytic strategies [15]. In that initial study, we demonstrated the ability to covalently couple streptokinase to the nanoparticle surface without reduction of bioactivity and showed that, despite the restrictive binding of streptokinase nanoparticles to the clot surface, plasmin penetrated the interstitium and affected rapid fibrinolysis, often with complete dissolution in 60 min.

In the present study, streptokinase, which is a bacterial-derived protein uniquely effective in humans, was replaced with human urokinase, and fibrin homing achieved by covalently coupling fibrin-specific monoclonal antibodies to the particle, rather than using avidin–biotin interactions. Although r-tPA or its direct analogues are most often used in humans for their thrombus specificity, these enzymes require conformational-induced activation achieved through direct fibrin binding. As a consequence, decorating the surface of each fibrin-targeted nanoparticle with r-tPA would result in inactivation of the majority of enzymes delivered to the thrombus due to a lack of direct fibrin binding, reducing the efficacy and efficiency of thrombolysis. In contradistinction, urokinase in the present study, coupled to the particle surface is constitutively active, thus maximizing the thrombolytic activity of agent. The thrombus specificity of the platform is achieved by the fibrin-specific monoclonal antibody. When compared with individually bound tPA molecules, the fibrin-targeted nanoparticles have great amplifying capacity to deliver hundreds of active urokinase molecules with each binding event.

The data in this study present a judicious, stepwise experimental approach leading to simultaneous coupling of maximal payloads of both anti-fibrin antibody (~160 kDa) and urokinase (~60 kDa) to the nanoparticle surface without impairing the functionality of either component due to chemical modification, particle coupling, or protein–protein steric interferences. While using 20 antibodies per particle, the maximum thrombolytic effectiveness was achieved with 200 urokinase molecules per particle with no change gained by doubling the surface enzyme density. Using this complex, the effectiveness for *in vivo* homing to thrombus created in dogs was compared between the fibrin-specific formulation and one targeted with an irrelevant IgG molecule. As clearly shown microscopically, fibrin-targeted urokinase nanoparticles heavily decorated the fibrin-rich surfaces of the electrically induced thrombus following intravenous injection into 10-kg beagles, whereas the nonspecifically targeted urokinase agents showed no association with intra-arterial thrombus.

Clearly, this study has limitations to be addressed through future experimentation. No extravasation of rhodamine-labeled thrombolytic particles was observed in the intact femoral artery, and only expected minor penetration was seen where the intima and internal elastic lamina had been ruptured with microthrombi deposition by inserting and securing the anode needle tip to the vessel. However, penetration into ischemic brain tissue with appropriate vascular constraint will need to be evaluated.

In the present study, a well-characterized murine fibrin antibody was utilized to home nanoparticles to thrombus to demonstrate the concept, but the efforts to humanize these homing ligands may not be justified if an equally specific and sensitive anti-fibrin peptide can be developed or identified. Currently, the specificity and binding affinity of the NIBSC antibodies [18] remain many-fold better than the best peptides reported.

Although the market for urokinase has diminished due to competition against superior, fibrin-activated thrombolytic enzymes, such as tPA, the use of human urokinase is necessary and warranted, if as we anticipate, the enzymatic efficiency of the targeted agent proves efficacious and safe. In fact, the hallmark opportunity for nanotechnologies in medicine is the rescue of shelved compounds through reduced dose-dependent and off-target toxicity, improved pharmacokinetics and biodistribution, and increased efficacy/unit drug by the concentrating effect of targeting. This nanolytic technology, although nascent, offers this potential for human urokinase in stroke.

Conclusion

This report describes the development, optimization and characterization of a fibrin-targeted urokinase nanoparticle, which could evolve into an alternative to r-tPA for use in acute ischemic stroke victims. Each nanoparticle delivers hundreds of urokinase molecules directly and specifically to fibrin–fibrils within the thrombus, concentrating plasmin generation proximal to the target. Although further research and development are required to produce a final candidate for clinical translation, many of the key design barriers have been addressed in these experiments. In comparison to r-tPA, the current standard of care, this nanolytic agent offers high vascular constraint, a simple administration protocol, and a lower total enzyme exposure. These collective benefits of this nanomedicine approach may offer an alternative therapeutic approach to decrease the morbidity and mortality prevalent among acute stroke.

Future perspective

In the near future, the number of stroke patients and their related healthcare costs are expected to rise. In western countries, the demographic changes in the population suggest an increase of 27% in the number of stroke patients per 1000 population in 2020 compared with 2000. Sophisticated advancement in safe and effective treatment approaches allowing more liberal patient stratification for use of thrombolytics could dramatically encourage greater earlier interventions. Efforts to shorten the time to cerebral reperfusion and diminish the current morbidity and mortality associated with stroke are essential for patients and the economic stability of world healthcare systems. A nanomedicine approach, using fibrin-targeted nanoparticles bearing thrombolytics, could provide a safe and effective agent for early intervention during acute ischemic stroke.

Bibliography

1. Morgenstern LB, Staub L, Chan W, et al. Improving delivery of acute stroke therapy: the TLL Temple Foundation Stroke Project. Stroke. 2002; 33(1):160–166. [PubMed: 11779906]

2. Wardlaw JM, Lindley RI, Lewis S. Thrombolysis for acute ischemic stroke: still a treatment for the few by the few. West J Med. 2002; 176(3):198–199. [PubMed: 12016247]
3. CASPR. Prioritizing interventions to improve rates of thrombolysis for ischemic stroke. Neurology. 2005; 64(4):654–659. [PubMed: 15728287]
4. Heiss WD. The concept of the penumbra: can it be translated to stroke management? Int J Stroke. 2010; 5(4):290–295. [PubMed: 20636712]
5. The National Institute of Neurological Disorders and Stroke rt-PA Stroke Study Group: tissue plasminogen activator for acute ischemic stroke. N Engl J Med. 1995; 333(24):1581–1587. [PubMed: 7477192]
6. Del Zoppo GJ, Saver JL, Jauch EC, Adams HP Jr. Expansion of the time window for treatment of acute ischemic stroke with intravenous tissue plasminogen activator: a science advisory from the American Heart Association/American Stroke Association. Stroke. 2009; 40(8):2945–2948. [PubMed: 19478221]
7. Hacke W, Kaste M, Bluhmki E, et al. Thrombolysis with alteplase 3 to 4.5 hours after acute ischemic stroke. N Engl J Med. 2008; 359(13):1317–1329. [PubMed: 18815396]
8. Engelman RM, Rousou JH, Dobbs WA. Fluosol-DA: an artificial blood for total cardiopulmonary bypass. Ann Thorac Surg. 1981; 32(6):528–535. [PubMed: 7316587]
9. Faithfull NS. Artificial oxygen carrying blood substitutes. Adv Exp Med Biol. 1992; 317:55–72. [PubMed: 1288172]
10. Winter P, Neubauer A, Caruthers S, et al. Endothelial $\alpha_v\beta_3$-integrin targeted fumagillin nanoparticles inhibit angiogenesis in atherosclerosis. Arterioscler Thromb Vasc Biol. 2006; 26(9): 2103–2109. [PubMed: 16825592]
11. Winter P, Caruthers S, Zhang H, Williams T, Wickline S, Lanza G. Antiangiogenic synergism of integrin-targeted fumagillin nanoparticles and atorvastatin in atherosclerosis. J Am Coll Cardiol Img. 2008; 1:624–634.
12. Winter PM, Schmieder AH, Caruthers SD, et al. Minute dosages of $\alpha_v\beta_3$-targeted fumagillin nanoparticles impair Vx-2 tumor angiogenesis and development in rabbits. FASEB J. 2008; 22:2758–2767. [PubMed: 18362202]
13. Zhou HF, Chan HW, Wickline SA, Lanza GM, Pham CT. $\alpha_v\beta_3$-targeted nanotherapy suppresses inflammatory arthritis in mice. FASEB J. 2009; 23(9):2978–2985. [PubMed: 19376816]
14. Alexandrov AV. Current and future recanalization strategies for acute ischemic stroke. J Intern Med. 2010; 267(2):209–219. [PubMed: 20175867]
15. Marsh J, Senpan A, Hu G, et al. Fibrin-targeted perfluorocarbon nanoparticles for targeted thrombolysis. Nanomedicine. 2007; 2(4):533–543. [PubMed: 17716136]
16. Tymkewycz PM, Creighton Kempsford LJ, Gaffney PJ. Generation and partial characterization of five monoclonal antibodies with high affinities for fibrin. Blood Coagul Fibrinolysis. 1993; 4:211–221. [PubMed: 7684615]
17. Edgell T, McEnvoy F, Webbon P, Gaffney P. Monoclonal antibodies to human fibrin: interaction with other animal fibrins. Thromb Haemost. 1996; 75(4):595–599. [PubMed: 8743185]
18. Raut S, Gaffney P. Evaluation of fibrin binding profile of two antifibrin monoclonal antibodies. Thromb Haemost. 1996; 76(1):56–64. [PubMed: 8819252]
19. Wahlgren N, Ahmed N, Davalos A, et al. Thrombolysis with alteplase for acute ischaemic stroke in the Safe Implementation of Thrombolysis in Stroke-Monitoring Study (SITS-MOST): an observational study. Lancet. 2007; 369(9558):275–282. [PubMed: 17258667]
20. Katzan IL, Furlan AJ, Lloyd LE, et al. Use of tissue-type plasminogen activator for acute ischemic stroke: the Cleveland area experience. JAMA. 2000; 283(9):1151–1158. [PubMed: 10703777]
21. Haley EC Jr, Thompson JL, Grotta JC, et al. Phase IIB/III trial of tenecteplase in acute ischemic stroke: results of a prematurely terminated randomized clinical trial. Stroke. 2010; 41(4):707–711. [PubMed: 20185783]
22. Hacke W, Albers G, Al-Rawi Y, et al. The Desmoteplase in Acute Ischemic Stroke Trial (DIAS): a Phase II MRI-based 9-hour window acute stroke thrombolysis trial with intravenous desmoteplase. Stroke. 2005; 36(1):66–73. [PubMed: 15569863]

23. Furlan AJ, Eyding D, Albers GW, et al. Dose Escalation of Desmoteplase for Acute Ischemic Stroke (DEDAS): evidence of safety and efficacy 3 to 9 hours after stroke onset. Stroke. 2006; 37(5):1227–1231. [PubMed: 16574922]
24. Qureshi AI, Harris-Lane P, Kirmani JF, et al. Intra-arterial reteplase and intravenous abciximab in patients with acute ischemic stroke: an open-label, dose-ranging, Phase I study. Neurosurgery. 2006; 59(4):789–796. [PubMed: 16915119]
25. Roman S, Knauer O, Cucuianu M. Clinical studies on α2 plasmin inhibitor. Med Intern. 1990; 28(1):73–81.
26. Thijs VN, Peeters A, Vosko M, et al. Randomized, placebo-controlled, dose-ranging clinical trial of intravenous microplasmin in patients with acute ischemic stroke. Stroke. 2009; 40(12):3789–3795. [PubMed: 19834019]
27. Alexandrov AV, Demchuk AM, Burgin WS, Robinson DJ, Grotta JC. Ultrasound-enhanced thrombolysis for acute ischemic stroke: phase I. Findings of the CLOTBUST trial. J Neuroimaging. 2004; 14(2):113–117. [PubMed: 15095555]
28. Alexandrov AV, Wojner AW, Grotta JC. CLOTBUST: design of a randomized trial of ultrasound-enhanced thrombolysis for acute ischemic stroke. J Neuroimaging. 2004; 14(2):108–112. [PubMed: 15095554]
29. Baron C, Aubry JF, Tanter M, Meairs S, Fink M. Simulation of intracranial acoustic fields in clinical trials of sonothrombolysis. Ultrasound Med Biol. 2009; 35(7):1148–1158. [PubMed: 19394756]
30. Meairs S, Culp W. Microbubbles for thrombolysis of acute ischemic stroke. Cerebrovasc Dis. 2009; 27(Suppl 2):55–65. [PubMed: 19372661]
31. Molina CA, Barreto AD, Tsivgoulis G, et al. Transcranial ultrasound in clinical sonothrombolysis (TUCSON) trial. Ann Neurol. 2009; 66(1):28–38. [PubMed: 19670432]
32. Hua X, Liu P, Gao YH, et al. Construction of thrombus-targeted microbubbles carrying tissue plasminogen activator and their *in vitro* thrombolysis efficacy: a primary research. J Thromb Thrombolysis. 2010; 30(1):29–35. [PubMed: 20155435]
33. Smith DA, Porter TM, Martinez J, et al. Destruction thresholds of echogenic liposomes with clinical diagnostic ultrasound. Ultrasound Med Biol. 2007; 33(5):797–809. [PubMed: 17412486]
34. Tiukinhoylaing S, Huang S, Klegerman M, Holland C, McPherson D. Ultrasound-facilitated thrombolysis using tissue-plasminogen activator-loaded echogenic liposomes. Thromb Res. 2007; 119:777–784. [PubMed: 16887172]
35. Shaw GJ, Meunier JM, Huang SL, Lindsell CJ, McPherson DD, Holland CK. Ultrasound-enhanced thrombolysis with tPA-loaded echogenic liposomes. Thromb Res. 2009; 124(3):306–310. [PubMed: 19217651]
36. Bi F, Zhang J, Su Y, Tang YC, Liu JN. Chemical conjugation of urokinase to magnetic nanoparticles for targeted thrombolysis. Biomaterials. 2009; 30(28):5125–5130. [PubMed: 19560812]
37. Ma YH, Wu SY, Wu T, Chang YJ, Hua MY, Chen JP. Magnetically targeted thrombolysis with recombinant tissue plasminogen activator bound to polyacrylic acid-coated nanoparticles. Biomaterials. 2009; 30(19):3343–3351. [PubMed: 19299010]

Executive summary

- In the present study, we have reported the development and characterization of fibrin-specific urokinase nanoparticle agent *in vitro* and *in vivo*.
- Urokinase was modified for coupling by the chemical conversion of amines to sulfhydryl groups, which slightly reduced the activity of the free enzyme.
- Simultaneous coupling of *N*-succinimidyl-*S*-acetylthioacetate (SATA)-modified anti-fibrin antibodies at up to 40 IgG molecules with 100 urokinase enzymes per particle produced effective clot dissolution versus control (no antibody) with no significant differences between the level of antibody added, suggesting that the independent bioactivities of the homing ligand and the enzyme were preserved.
- Further increasing the density of urokinase or streptokinase enzymes co-coupled to the surface of the nanoparticles from 100 to 400 molecules in the presence of 20 anti-fibrin antibodies produced greater clot dissolution with increasing kinase surface density.
- For streptokinase nanoparticles, the overall dissolution of plasma clots was less than for the urokinase nanoparticles but improvement ($p < 0.05$) in fibrin degradation was noted for each increase in enzyme density. For urokinase, the best dissolution was measured for nanoparticles with 200 or 400 urokinase molecules attached.
- Comparing fibrin clot dissolution rates between free SATA-modified urokinase and urokinase covalently coupled to fibrin-targeted nanoparticles revealed no difference in the rate of clot degradation over time. In contradistinction, free SATA-modified streptokinase had significantly lower fibrin dissolution rates after 30 min of incubation than the fibrin-targeted streptokinase nanoparticles, which was consistent with our previous report. After 60 min, however, the rate of clot dissolution for the streptokinase nanoparticles was less ($p < 0.05$) than the free enzyme for unclear reasons.
- Microscopic examination of rhodamine-labeled urokinase nanoparticles clearly showed that the fibrin-targeted agent decorated the serpentine periphery of the intraluminal thrombus analogous to the fibrin pattern obtained with Carstair's staining. Moreover, minute mural deposits of microthrombus associated within the intimal disruption from the anodal injury procedure revealed high-intensity fluorescent signal from the rhodamine-labeled fibrin-targeted urokinase particles, indicating that homing efficacy of this agent was not restricted to large intra-luminal thrombus. The nonspecifically targeted agent had negligible binding to fibrin-rich femoral thrombus.
- Collectively, these results demonstrate a fibrin-specific urokinase nanoparticle formulation with high fibrinolytic activation activity that can be effectively and specifically targeted to intra-arterial thrombosis in a large animal model.

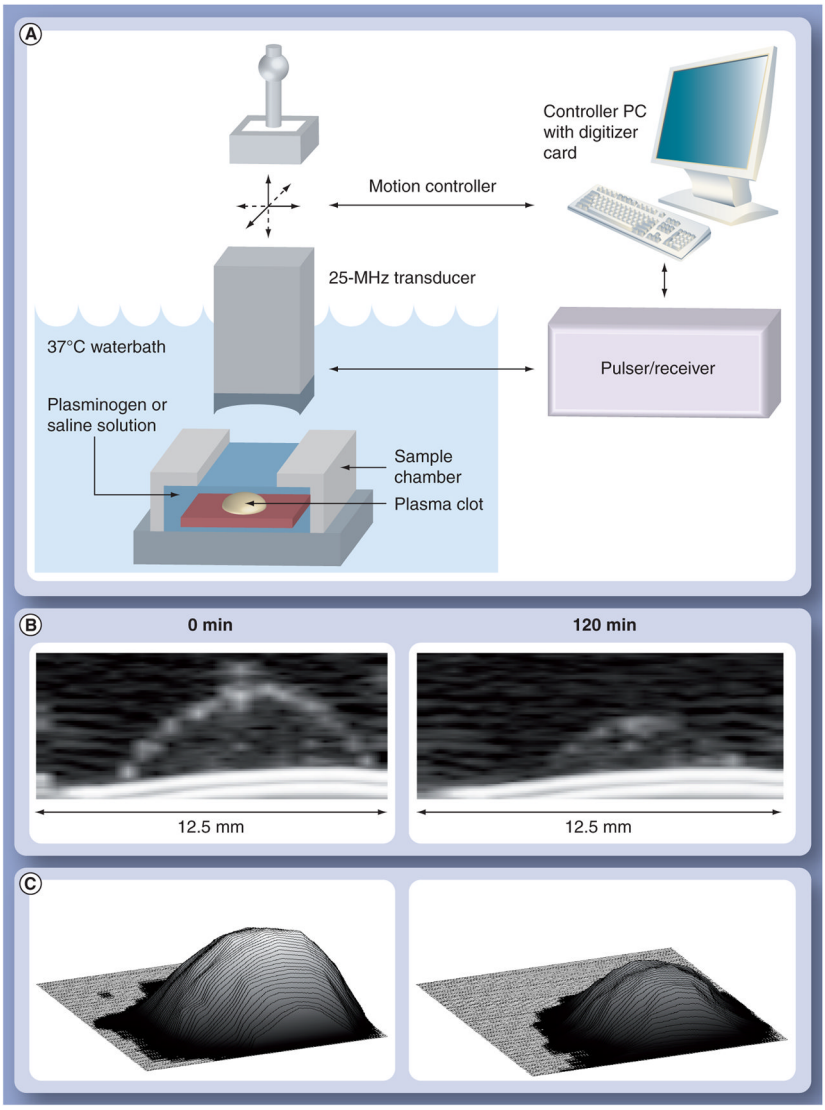

Figure 1. Clot digestion monitored with ultrasound

(A) Acoustic microscopy setup for imaging *in vitro* clot dissolution. **(B)** Example cross-sectional ultrasonic backscatter images of plasma clot targeted with thrombolytic nanoparticles at baseline (0 min) and after 120 min of exposure to plasminogen solution. **(C)** Volume reconstructions of plasma clot at baseline (0 min) and after 120 min digestion.

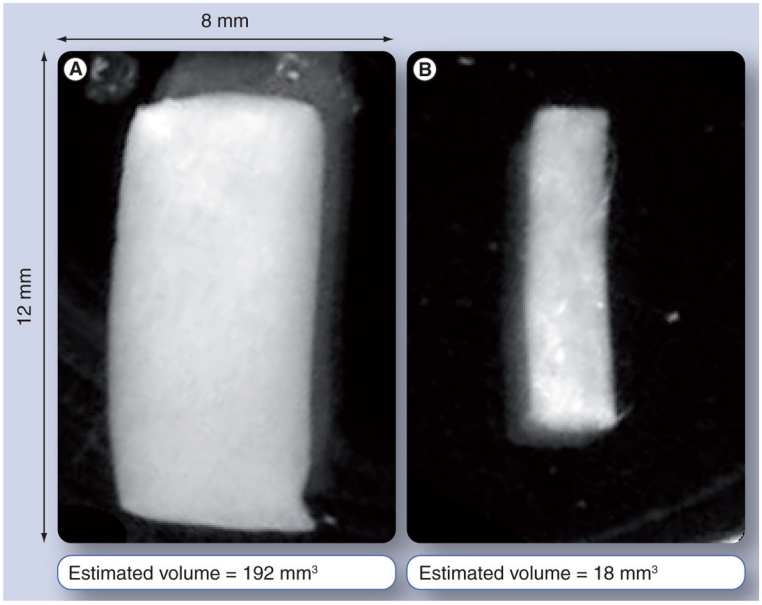

Figure 2.
Optical photographs of a tubular plasma clot targeted with thrombolytic nanoparticles at (A) baseline and (B) after 90 min lytic activity

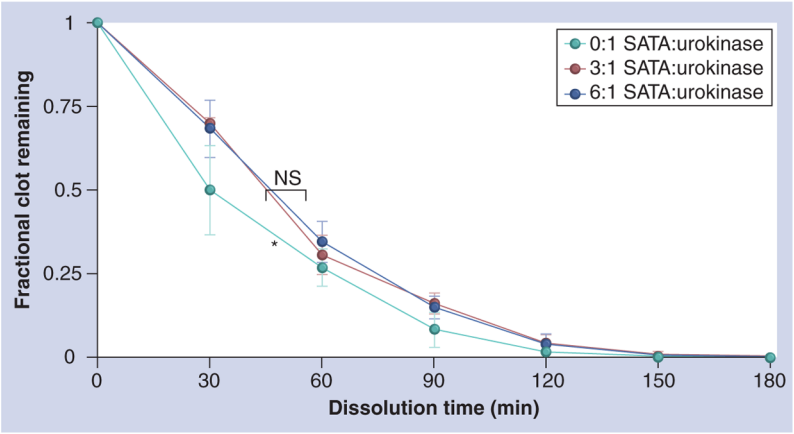

Figure 3. Clot volume as a function of time when exposed to free and *N*-succinimidyl-*S*-acetylthioacetate-modified urokinase

Sulfhydryl functionalization of urokinase at ratios of 3:1 and 6:1 SATA-modified sites per enzyme significantly decreased the overall enzymatic activity relative to free (0:1). *$p < 0.05$. NS: Nonsignificant; SATA: *N*-succinimidyl-*S*-acetylthioacetate urokinase.

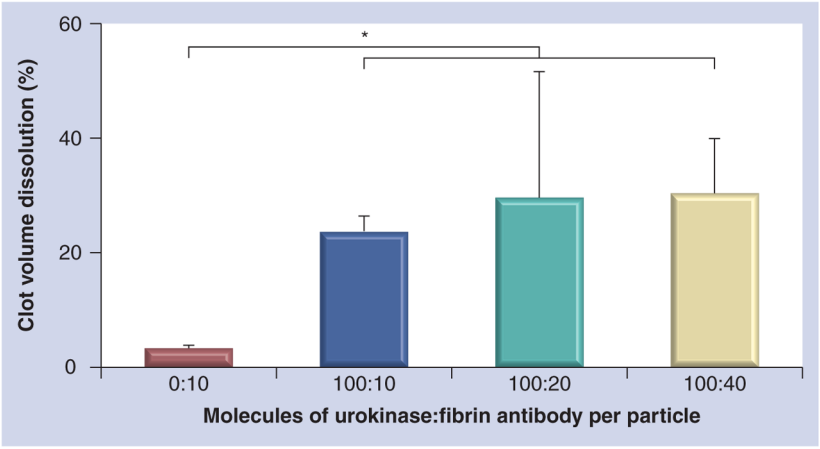

Figure 4. Effect of antibody presentation density in the presence of urokinase at nominal number of anti-fibrin antibodies at zero, 10, 20 and 40 per particle

Antibodies were simultaneously coupled to the particle along with 100 urokinase molecules presenting 0:10, 100:10, 100:20 or 100:40 urokinase:antibody per particle. *$p < 0.05$.

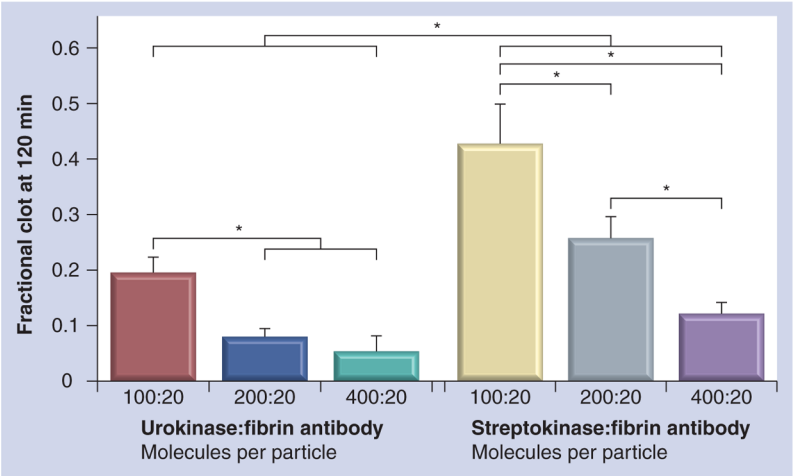

Figure 5. Differential effect of urokinase and streptokinase on fibrinolysis when varying the number of enzymes (at levels of 100, 200 and 400) per particle in the presence of 20 1H10 antibodies previously coupled to particle

*$p < 0.05$.

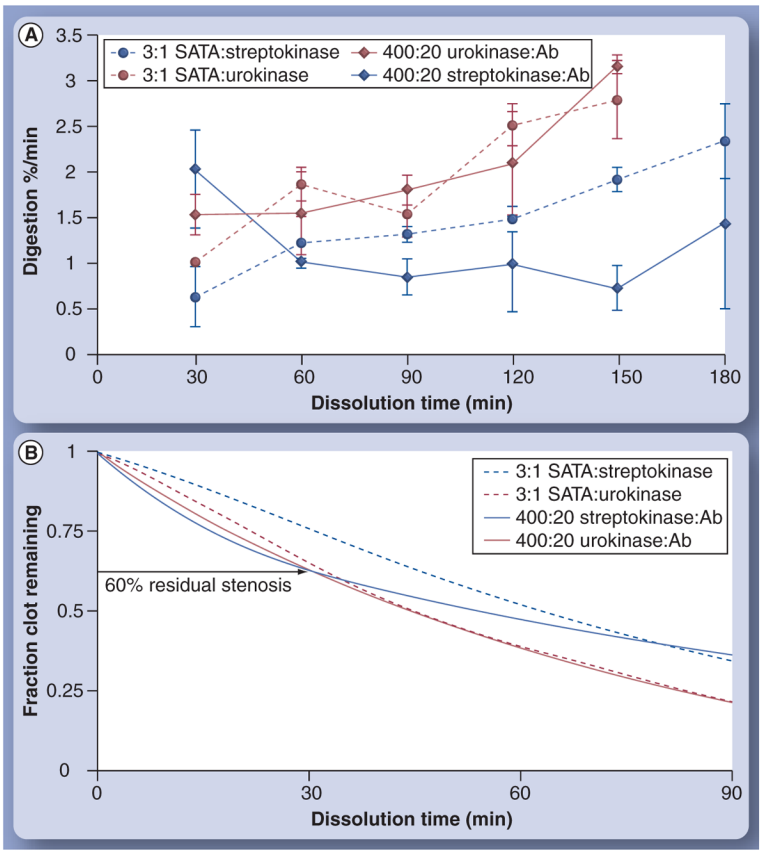

Figure 6. Clot digestion rates for functionalized enzymes with and without particles

(A) Comparison of the rates of clot dissolution for fibrin-targeted streptokinase and urokinase functionalized nanoparticles (400:20) with equivalent concentration of free 3:1 SATA-functionalized enzymes. **(B)** Modeled rate data of fractional clot remaining as a function of time. Ab: Antibody; SATA: *N*-succinimidyl-*S*-acetylthioacetate.

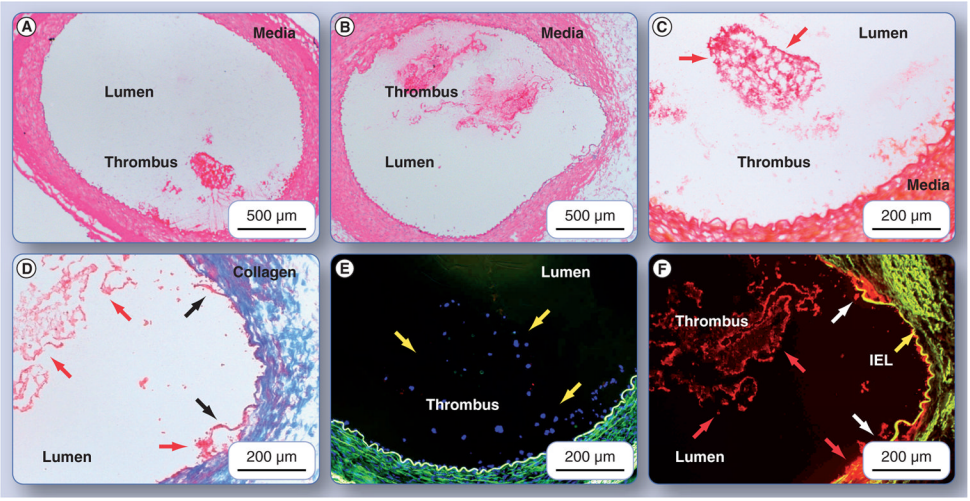

Figure 7. Canine arterial sections with thrombus exposed to fibrin-targeted or irrelevantly targeted nanoparticles

Hematoxylin and eosin-stained femoral artery segment from **(A)** a dog administered irrelevant-targeted urokinase-loaded particles, and **(B)** a dog given fibrin-targeted, urokinase-loaded particles, show anodal injury-induced thrombus attached to the femoral wall. Slice shown in **(B)** was fortuitously obtained near the needle injury site and revealed disruption of the intima, media and internal elastic lamina (highlighted with dark arrows **[D & F]**). Carstair's staining of fibrin is shown in (**[C & D];** which are magnified portions of **[A & B]**, respectively), revealed an abundance of the target protein in both thrombi. Fibrin is shown in bright red, platelets in gray–blue to navy, collagen in bright blue, muscle in red and red blood cells in yellow. Note in **(D)** that the medial layer has been completely disrupted by the needle injury and collagen is primarily visible in this portion of the vessel wall. Fluorescent microscopic examinations of the thrombi that show the fibrin-targeted urokinase nanoparticles labeled with rhodamine **(F)** were bound along the serpentine surface of thrombus in a pattern consistent with the fibrin deposits revealed by the Carstair's stain in **(D)**. In contradistinction, only negligible binding of the irrelevant-targeted urokinase particles labeled with rhodamine was observed **(E)**, despite a prominent accumulation of the target protein show in **(C)**. IEL: Internal elastic lamina.